X-ray imaging tests of Constellation-X SXT mirror segment pairs

S. Owens Rohrbach[*a], T. J. Hadjimichael[b], L. Olsen[b], Kai-Wing Chan[c], J. P. Lehan[c], P. B. Reid[d], R. Petre[a], S. L. O'Dell[e], T. T. Saha[a], W. W. Zhang[a]

[a] Goddard Space Flight Center, NASA, Greenbelt, MD 20771
[b] Ball Aerospace, 1616 McCormick Drive, Upper Marlboro, MD 20774
[c] Center for Research and Exploration in Space Science and Technology, NASA Goddard Space Flight Center, and Department of Physics, University of Maryland, Baltimore County
[d] Harvard–Smithsonian Center for Astrophysics, 60 Garden Street, Cambridge, MA 02138
[e] Marshall Space Flight Center, NASA, Huntsville, AL 35812

ABSTRACT

The Constellation-X Spectroscopy X-ray Telescope (SXT) is a segmented, tightly nested Wolter-I telescope with a requirement of approximately 12.5″ half-power diameter (HPD) for the mirror system. The individual mirror segments are 0.4-mm thick, formed glass, making the task of mounting, alignment and bonding extremely challenging. Over the past year we have developed a series of tools to meet these challenges, the latest of which is an upgrade to the 600-meter x-ray beam line at GSFC. The new facilities allow us to perform full-aperture and sub-aperture imaging tests of mirror segment pairs to locate the source of deformations and correlate them with our optical metrology. We present the optical metrology of the axial figure and Hartmann focus, x-ray imaging performance predictions based on analysis of the optical metrology, and both full-aperture and sub-aperture x-ray imaging performance of test mirror segment pairs at 8.05 keV.

Keywords: X-ray optics, x-ray imaging, metrology, performance prediction, integration and test

1. INTRODUCTION

The Constellation-X Spectroscopy X-ray Telescope (SXT) will be the largest x-ray telescope ever built. The design requires the production of over 100 m^2 of precision mirror surface. Technology development has concentrated on a multi-step progression to prove our ability to manufacture, characterize, mount, align, and test thin, segmented Wolter-I mirrors. At this stage, we have demonstrated the ability to manufacture,[1] characterize,[2] and mount[3] test-mirror segments, and to maintain image quality near that of the current mission requirements. This report demonstrates the next step in the process, which is to prove that the current manufacturing method yields mirrors of high quality and that their x-ray imaging is consistent with predictions based on optical metrology, and similarly near the mission's imaging requirement. We present, for a mirror segment pair, the optical metrology, x-ray imaging performance prediction, and experimental full- and sub-aperture x-ray imaging results. These demonstrate imaging resolution of 15″ half-power diameter (HPD).

2. EXPERIMENTAL SETUP

Detailed elsewhere in these proceedings,[3] we mounted the test mirror segments on our "cradle and mattress" system. The intention of this mount is to provide a means to evaluate mirror segments in an orientation in which they could be x-ray tested. It is not a flight-like mount, but provides an opportunity to test imaging quality without the difficulties, cost, and long manufacturing time of building and testing a flight-like design. Nonetheless, it is a large step toward demonstrating the next significant goal of high quality imaging from a mirror segment pair in a flight-like mount.

[*] Scott.O.Rohrbach@nasa.gov; Code 551, NASA/GSFC, Greenbelt, MD 20771.

Space Telescopes and Instrumentation 2008: Ultraviolet to Gamma Ray, edited by Martin J. L. Turner, Kathryn A. Flanagan, Proc. of SPIE Vol. 7011, 701134, (2008) · 0277-786X/08/$18 · doi: 10.1117/12.789838

3. OPTICAL METROLOGY

As noted elsewhere in these proceedings,[3] we obtained a full set of optical metrology of the mirror segments during integration on the mattress system. These data consist of a full-aperture focused image, a Hartmann map using 26 points across the azimuth of the mirror(s), and 26 axial profiles measured via normal-incidence interferometry. Although we measured each of these at various stages of the alignment, for this report, we present the relevant data taken just prior to transporting the mirror pair to the x-ray beam line. Figure 1 displays the surface maps (built using the 26 axial profiles without any tilt or piston adjustment) for the primary and the secondary mirror segments. The surface heights represent deviations from a perfect cone, not from the prescription—approximately a quadratic with a peak-to-valley (P–V) magnitude of 1.1 μm (sagittal depth, or "sag") along the axial length.

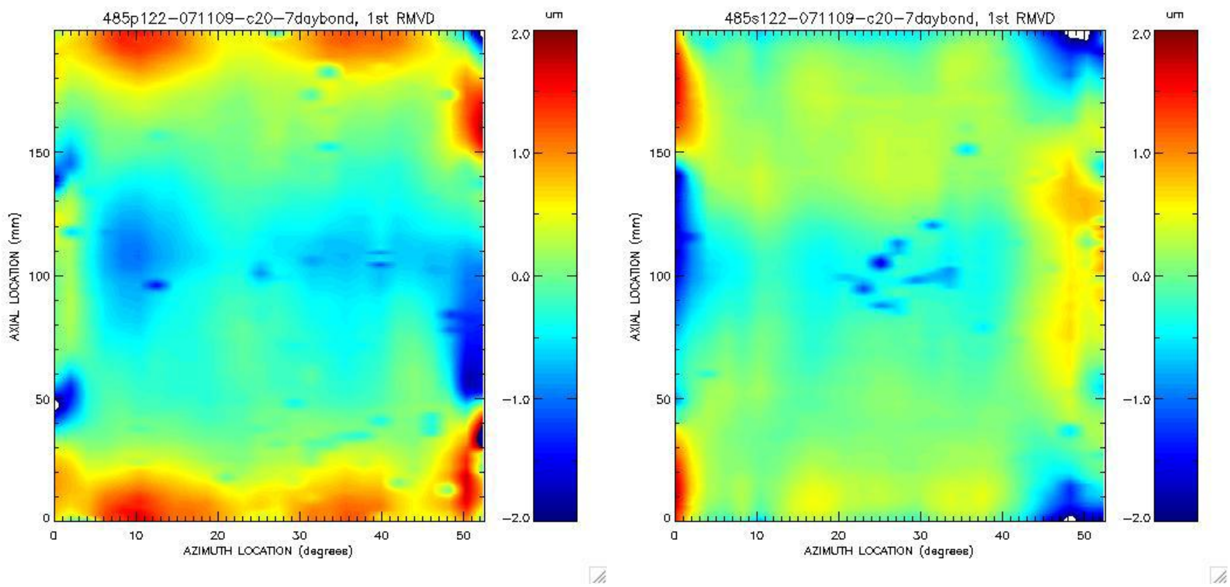

Figure 1. Surface maps for (left panel) the primary and (right panel) the secondary mirror segments. The surface heights represent the deviation from a perfect cone.

As evident in Figure 1, most of the area of each mirror segments has approximately the correct concave axial curvature, ≈1.1 μm P–V. The outer few degrees on either side shows non-desirable figure—distortions caused by the tack bonds holding the mirror to the cradle—at the 50 and 150 mm axial positions of either side of the mirror. In our current flight housing concept, mounting and bonding occurs on the azimuthal edges where mounting structure will block the x rays, thus preventing the distorted areas from contributing to the telescope's point spread function (PSF).

Figure 2 shows the focused optical images (a) from the primary mirror segment, (b) from the secondary mirror segment, and (c) from the pair. We obtained each image at the nominal focal length of the respective mirror or pair—16.8 m for the primary, 5.53 m for the secondary, and 8.4 m for the aligned pair. The plate scales of each of the images are not equal, so we have adjusted the scales to make the images approximately the same size for comparison. We use visual inspection of the images to help in alignment and "tuning" of the mirror shape on the mattress system. While the images for the primary and for the pair show very good quality, that for the secondary indicate an error in its focal length.

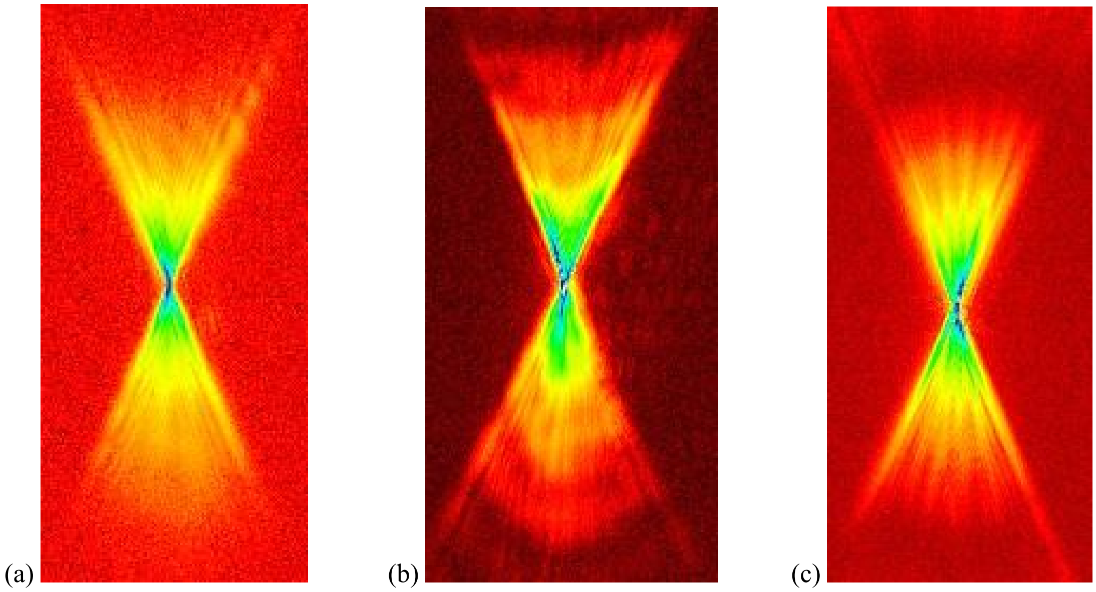

Figure 2. Full-aperture optical images from (a) the primary mirror segment, (b) the secondary mirror segment, and (c) the aligned primary–secondary pair. These images are each at the best focus of the respective mirror segment or pair.

The optical Hartmann map in Figure 3 illustrates how much the pointing error changes with azimuth for the combined primary–secondary mirror segment pair. This azimuthal variation in pointing direction contributes 3.0″ root-mean-square (RMS) diameter (1.3″ HPD) to the full-aperture image blur.

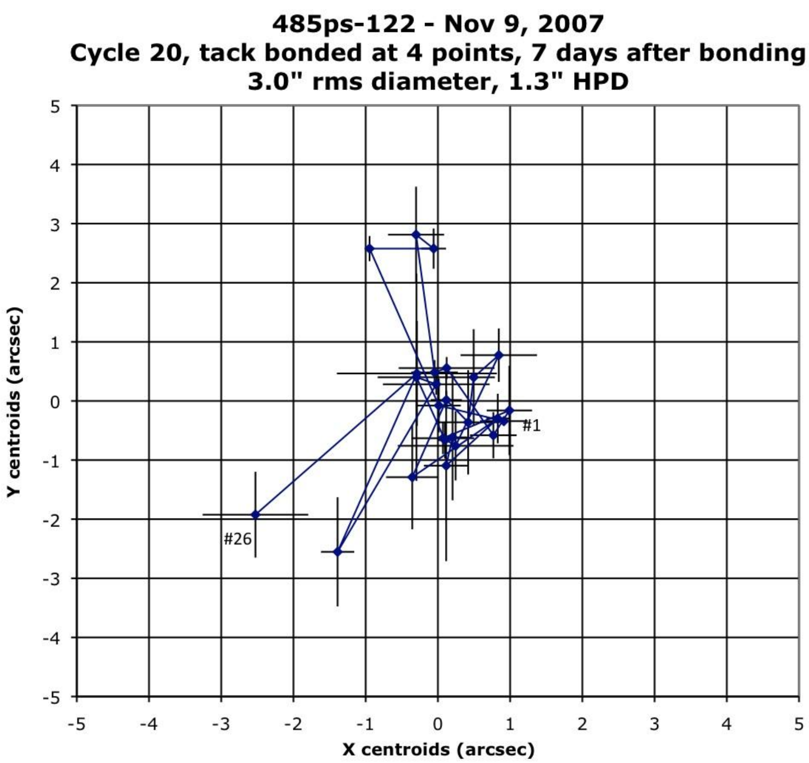

Figure 3. Optical Hartmann map of the aligned primary–secondary pair. The map displays the relative pointing errors for the sampled azimuths. The map shows a 3.0″ RMS diameter error and a 1.3″ HPD.

4. PERFORMANCE PREDICTION

There are a variety of ways to use the optical metrology data above to predict accurately the x-ray imaging performance of the aligned mirror pair. We have chosen to calculate the performance directly from the diffraction integral on a profile-by-profile basis, at the test x-ray wavelength (1.54 Å). The prediction includes both the effects of figure errors (Figure 1) and those of measured micro-roughness on the primary and secondary mirrors. We then position the centroid of the imaging stripe in the image plane where the corresponding optical Hartmann point is located. This permits synthesizing the full-aperture image without building a full-surface model for each mirror segment, a process that may introduce artifacts or miss features as a result of fitting errors.

Figure 4 displays the simulated x-ray image of the mirror pair for the surface deviations shown in Figure 1. The expected imaging quality for the full aperture is 20.1″ HPD. Because the x-ray beam in our facility only spans ≈47° for the mirror segments being tested, we ray trace only profiles within the central 47° to synthesize a single experimental image. The expected image quality for this central region is 16.8″ HPD.

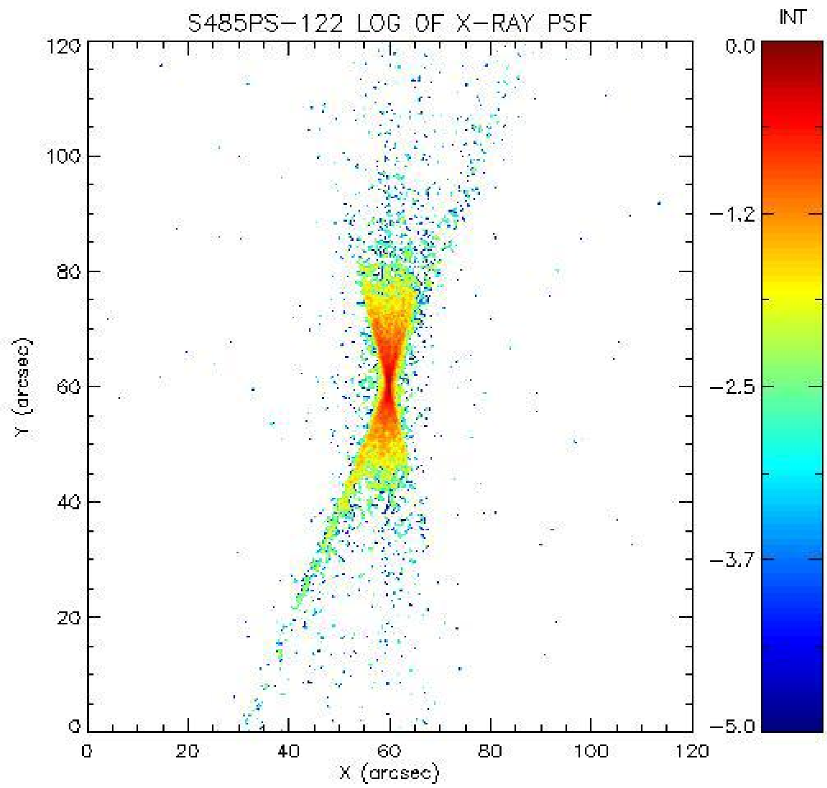

Figure 4. Predicted x-ray image from the aligned 485-122 mirror pair, based upon the surface metrology and the optical Hartman map. The predicted imaging quality is 16.8" HPD for the (central 47°) full aperture.

Given the limitation of the beam line to cover only 47° of a mirror segment pair, another useful characterization method is to plot the predicted HPD as a function of azimuth. This does not include imaging errors associated with relative tilt versus azimuth errors (ΔΔr); however,the contribution of these errors to the overall image is small for this case. As evisdent in Figure 5, the central region of the mirror pair should image at around 15” HPD, while the outer azimuths suffer from distortions introduced by the tack bonding.

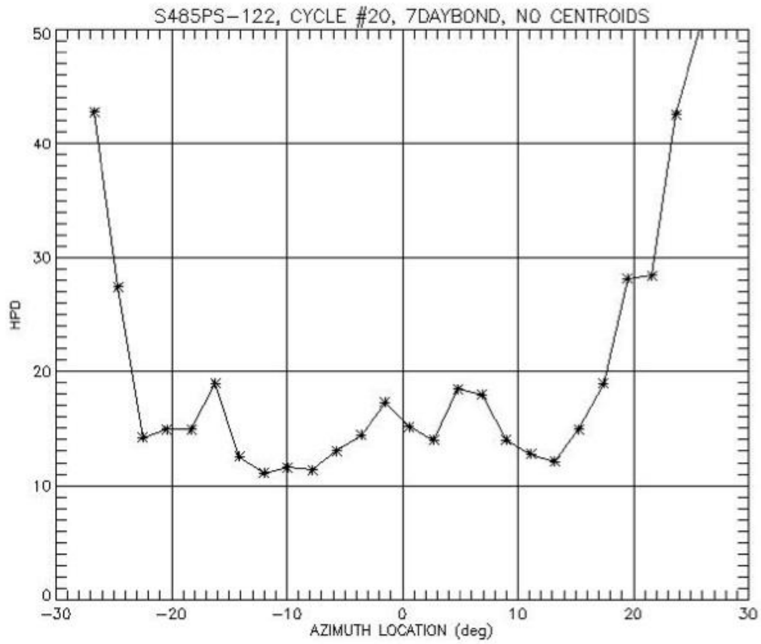

Figure 5. HPD versus azimuth for the 485-122 mirror pair, as determined by ray tracing the corresponding primary–secondary axial profiles.

5. X-RAY IMAGING TESTS

After completing the optical metrology and performance predictions, we transported the mirror pair to a new x-ray beam line at Goddard Space Flight Center.[4] In brief, the x-ray source lies ≈600 meters from the optics test chamber, joined by a vacuum pipe evacuated to ≈1 mTorr. This allows testing at x-ray energies as low as 1 keV using relatively low-power sealed-tube x-ray sources. The source used for this first test is an Oxford X-ray Technologies model 5011 with a copper anode, producing characteristic x rays at 8.05 keV (Kα) and at 8.9 keV (Kβ), with a broad Bremsstrahlung continuum. A 0.125-mm Be window highly attenuates X rays below ≈2.5 keV; thus the copper L-line is undetected. The spot size of this source is less than 0.1 mm, 0.034″ at 600 m—i.e., effectively an ideal point source for the purposes of these tests. When operated at our nominal settings of 35 kV and 0.5 mA, and focused from the full aperture of the test mirror pair, the detected count rate is approximately 1 photon/s.

The detector is a Princeton Instruments x-ray CCD with 1024×1024 13-μm pixels, operated at about -100° C. For these measurements, we ran the CCD in intensity (charge-collection) mode—i.e., we simply exposed the camera for long periods and read out the total intensity in each pixel. In future tests, we shall use a photon counting mode, tagging each photon with its energy and position in the focal plane. This will reduce our sensitivity to undesirable background effects and allow us to examine only characteristic photons, or the entire spectrum, at will. We located the CCD 8.52 m behind the primary–secondary intersection plane, the finite-conjugate focus for an 8.40-m focal length at 600-m source distance.

We mounted the mirror pair on a series of stacked stages: At the base is a 2-axis rotation stage that controls the pitch and yaw of the mirror pair in the beam; under each mirror segment is a 5-axis stage that provides pitch, yaw, and translation in each direction, with respect to the other mirror segment. During optical metrology, we used this combination of stages to align the mirror segments to one another and to maintain that alignment at reasonably good accuracy during transportation. However, we needed some re-alignment of the pair after installation in the x-ray facility using the secondary mirror segment 5-axis stage.

To obtain initial coarse alignment, we placed the CCD in line with the mirror pair, and acquired x-ray shadow images while tilting the pair until the relative shadow widths and separation was consistent with expected values. Then, we translated the CCD to the expected focus position, and precisely aligned the individual mirror segments with respect to each other and the pair with respect to the x-ray beam.

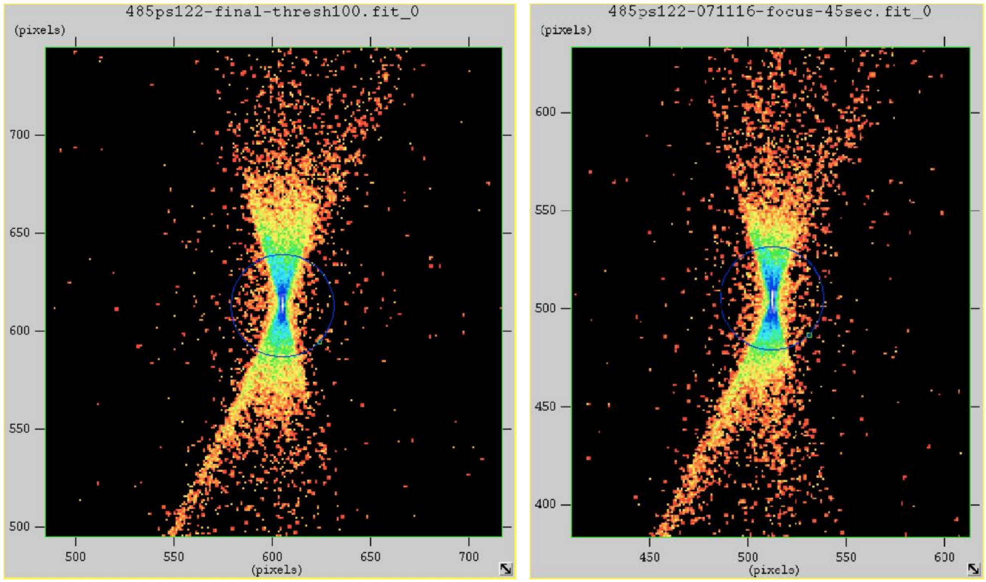

Figure 6. Day-1 (left) full-aperture x-ray image from the aligned 485-122 mirror pair; Day-2 (right) full-aperture image. The circle in each image indicates the HPD ring for the (central 47°) full aperture.

After achieving the best alignment of the pair, we recorded a full-aperture image. Because the beam is slightly smaller in diameter than the full span of the mirror pair, "full aperture" images cover a ≈47° span of the 54° mirror segments. The full-aperture image (Figure 6, left panel) matches very accurately the predicted image (Figure 4)—including the "flare" at the 7 o'clock position, arising from a local tilt error near the edge of the secondary mirror. On the second day of testing, after another series of re-alignments, we recorded a second full-aperture image (Figure 6, right panel). The HPDs for the first and second day images are 16.6″ and 14.7″, respectively. Figure 7 shows the encircled-energy distributions for the two images, with respect to each image's centroid.

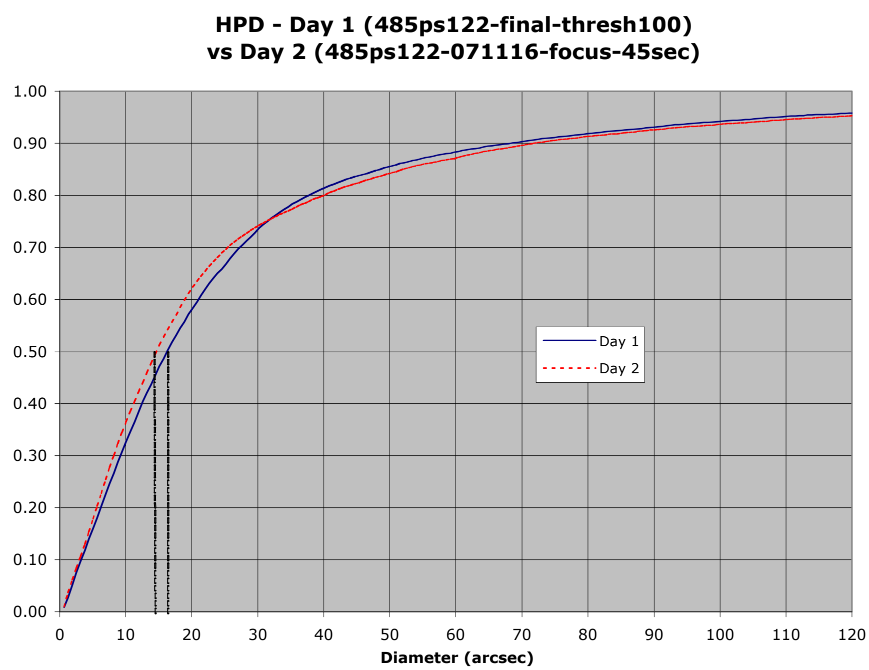

Figure 7. Encircled energy curves for the two (central 47°) full-aperture images shown in Figure 6.

After concluding the full-aperture tests, we inserted a 2°-wide scanning mask in front of the mirror pair. The mask scanned across the mirror pair in 2° steps, with a 2-minute exposure at each position, to enable quantifying the imaging quality at each azimuthal position. Figure 8 shows sub-aperture images from two extreme positions of the mask that yielded significant counts. In Figure 9 we plot the centroid of each of the sub-aperture images, to produce an x-ray Hartmann map. The scatter of the image centroids is 2.0″ radius RMS.

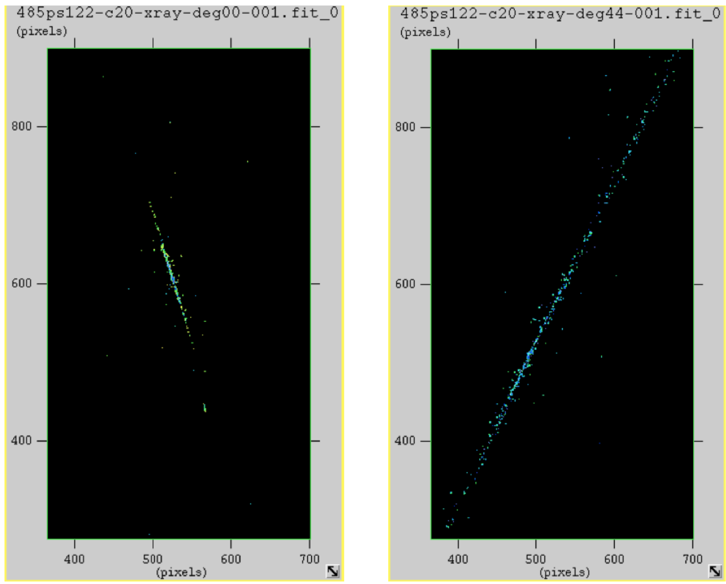

Figure 8. Example x-ray images taken with a 2° scanning aperture.

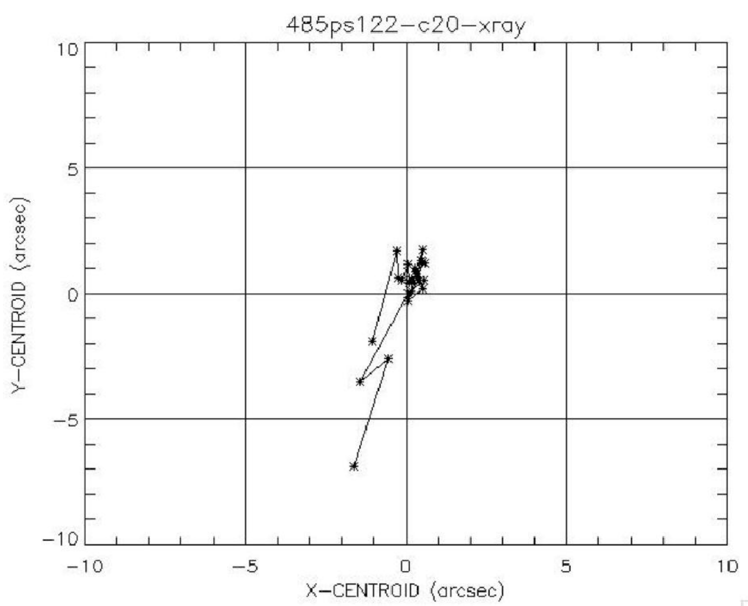

Figure 9. X-ray Hartmann map generated by plotting the centroid of each of the 2°-aperture x-ray images.

Figure 9 compares predicted and experimental imaging quality. The agreement between the experimental and predicted performance is generally very good—other than in the 43°–51° range, where a large measured sag error leads to a prediction of high HPD for that region. We believe that the mirror sag changed during transportation to and pump down in the x-ray beam line.

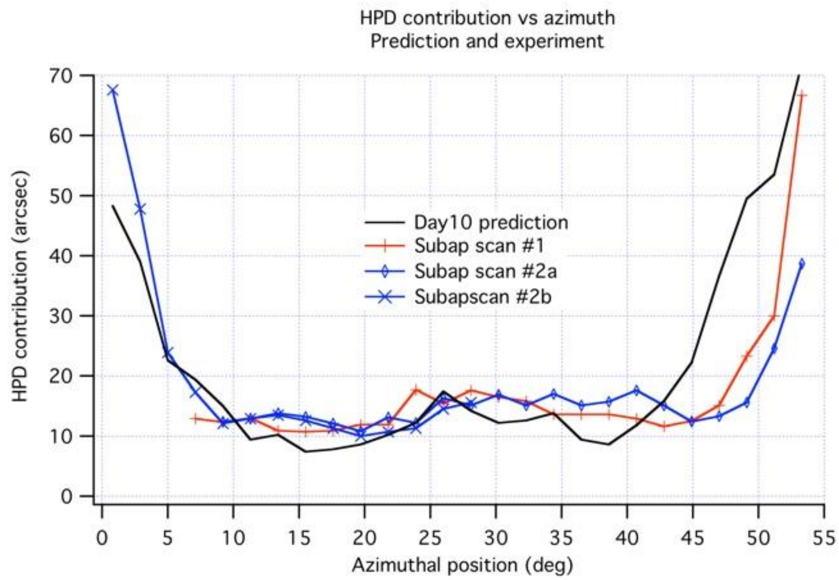

Figure 10. Comparison of predicted imaging quality versus azimuth with that observed. Solid (black) line denotes predicted HPD; line (red) with +, sub-aperture scan #1; lines (blue) with ♦ and ×, two overlapping sub-aperture scans to span the entire azimuthal range of the mirror pair.

6. CONCLUSIONS

We successfully manufactured, characterized, mounted, aligned, and x-ray tested a flight-scale Constellation-X SXT mirror segment pair. We utilized a performance prediction based upon optical metrology of the surface to build a model, from which we calculated the x-ray imaging quality, both for the full aperture and as a function of azimuth. The experimental data show performance very similar to that predicted, and demonstrate that the mirror quality and our ability to hold mirror segments as a semi-rigid body, results in an image near the mission requirement of ≈11″ HPD. Further experiments will repeat these tests, and we are in the process of moving towards rigidly mounting multiple mirror segment pairs in a quasi-flight-like housing that can pass environmental tests with the imaging quality intact.

7. ACKNOWLEDGEMENTS

We thank Keith Gendreau for his leadership and determination in building the x-ray beam line facility used in this work. We are also thankful for financial support from the Constellation-X Project Office, the GSFC Internal Research and Development fund, the NASA Astronomy and Physics Research and Analysis chapter of the ROSES program.

REFERENCES

[1] W. W. Zhang, *et al.*, “Constellation-X Mirror Technology Development”, Proc. SPIE 7011, Paper 7011-2 (2008).

[2] J. P. Lehan, *et al*., “Some considerations for precision metrology of thin x-ray mirrors”, Proc. SPIE 7018, Paper 7018-42 (2008).

[3] T. Hadjimichael, *et al.*, “Bringing a Constellation-X Mirror Pair to First Light in the X-Ray Band”, Proc. SPIE 7011, Paper 7011-40 (2008).

[4] `http://lheawww.gsfc.nasa.gov/~kcg/beamline/home.html`